

# MINIFLOAT: A Novel Concept of Minimal Floating Platform for Marginal Field Development

*C.A. Cermelli, D.G. Roddier, C.C. Busso*  
Marine Innovation & Technology  
San Francisco, CA, USA

## ABSTRACT

This paper describes a new type of minimal floating offshore platform, named MINIFLOAT, suitable for developing deepwater marginal fields. The paper covers the design methodology and hydrodynamic analysis of the platform. The numerical method used to determine the floater dynamics is presented. Results of the platform response are given for a specific case.

The platform described in this paper can be used in a number of ways to support various equipment used in the production of oil and gas from deep and ultra-deep water hydrocarbon fields:

- support and control to a subsea wellhead, including chemical injection, hydraulic power, telecommunication
- host water-injection equipment to assist field production
- host first stage separation equipment to allow long offsets to hub/shore
- provide power supply to heated flowlines, multiphase pumps or other subsea installations.

This new concept enables safe and cost-efficient development of marginal fields in deep and ultra deep water. It allows application of advanced subsea technologies to reduce field development cost, while maintaining a surface "presence" for reduced cost, enhanced reliability and ease of maintenance.

**KEY WORDS:** Offshore platform, Marginal fields, Subsea equipment

## INTRODUCTION

As the demand for hydrocarbons in the next 10 years is expected to increase by as much as 5 percent a year, and as very large oil and gas fields are less likely to be found, oil and gas companies are looking into means of developing their proven smaller reserves. Significant exploration activities have taken place in recent years in the deep waters of the Gulf of Mexico resulting in numerous discoveries. However, many of these fields do not contain sufficiently large amount

of oil or gas to justify the expenses of a stand-alone field development, such as a production platform and pipeline infrastructure.

To reduce the threshold of recoverable oil or gas, new technologies are being developed in the field of subsea equipment and long tie-backs. However, even the most recent advances still require either power generation or chemicals to be supplied to the wellhead. A number of functionalities (chemical storage, power generation, communication, etc.) can be performed more reliably and economically at the surface provided a low cost, stable floater is available.

MINIFLOAT unique design combines features of a very small semi-submersible platform and a large water-entrapment plate at the keel, to provide a small, multi-function floating platform with excellent motion characteristics. The platform can economically support surface equipment required for the successful development of marginal fields.

Currently, providing surface support to deepwater developments is achieved by three main types of platforms.

## Review of existing floaters

Semi-submersible platforms are moored floating structures made of multiple columns connected by pontoons. They were originally developed to conduct drilling operations in deep water. Semi-submersible platform displacement exceeds 20,000 tons in order to provide sufficient stability during extreme weather events. These platforms can therefore carry a large payload, in excess of several thousands tons, but consequently their cost is high. Because of their large displacement, the required mooring system is very large and increases significantly in size and cost with water depth.

Spar-type concepts consist of a single column moored to the sea bed using anchors and mooring lines. Initially, the spar was a deep draft vertical cylinder. The deep draft minimizes heave motion, but increases the system cost. The truss spar, and the recently developed cell spar are based on technology advances that reduce the size and cost of the platform. An inherent problem of the single column concept is that it suffers greatly from Vortex Induced Motions (VIM), a physical phenomena causing the platform to oscillate perpendicularly to the dominant current direction. These large oscillations decrease the

fatigue life of the mooring system and cause operational concerns. Common mitigation devices are strakes, which reduce correlation of vortex formation along the hull. Strakes do not always perform as expected, and increase the wetted surface of the platform hence the strength requirements of the mooring system. The spar installation and fabrication costs are high because of the large size of the hull, and the requirements to upend the structure and integrate the topsides offshore.

Finally, tension leg platform (TLP) concepts have also been used to support deepwater facilities in depth extending to almost 5,000 ft. TLP are connected to the sea-bed by a set of vertical steel pipes, or tendons, which provides excellent motion response in heave and pitch. Various TLP concepts have been used, such as the Atlantia Sea-Star, ABB extended TLP, Modec mini-TLP, and the conventional 4 or 6 columns TLP for large payloads. TLP cannot easily be extended to the ultra-deepwater range - water depth greater than 5,000 ft - due to the requirement to keep the heave natural period smaller than the waves, usually less than 4 seconds. Installation of the tendons is very costly. In addition, the tendons are subject to Vortex-Induced Vibrations (VIV), which makes their design challenging (ABS, 2003 and Shell, 2003).

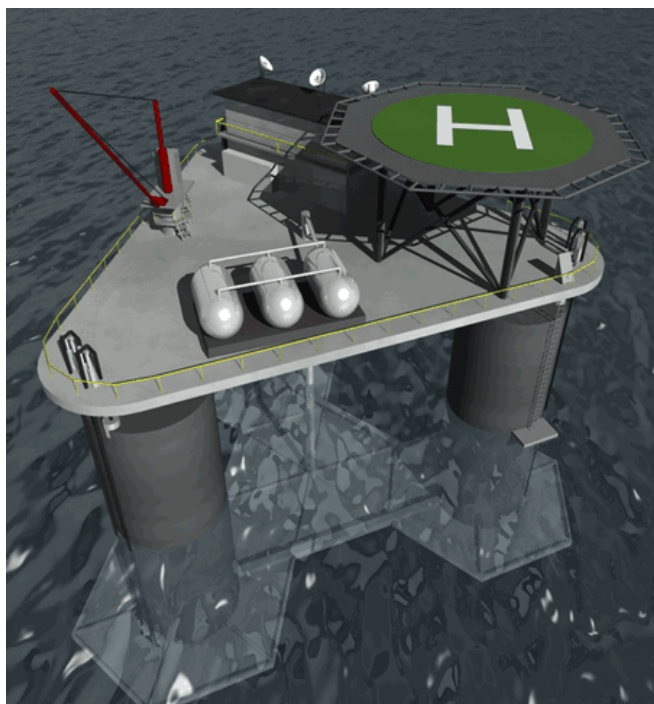


**Figure 1. MINIFLOAT platform**

MINIFLOAT, shown in Figure 1, has been optimized to carry small payloads in deep and ultra-deep waters. Due to its small size, the mooring system consists of small size wire ropes or synthetic lines. Its multi-column design is not subject to VIM problems. The large water-entrapment plate located at the keel improves the platform response significantly. It has similar features as the truss spar heave plates which enhance the motion performance, as shown by Tao et al, 2000, O’Kane et al, 2002, and Thiagarajan, 2002. The damping provided by the plate reduces the motions, while the additional added mass and added moment of inertia shift the platform response above the typical wave range. The MINIFLOAT water-entrapment plate has also been optimized to minimize the pitch response. This is achieved by extending the plate area on the outside of the columns. The shape of

the plate has also been designed to minimize the lift.

Computational fluid dynamics (CFD) methods are generally used to predict the hydrodynamic loads on heave plates. However, numerical tools predictions still need to be calibrated through model tests when viscosity and high order wave forces are present. From these tests, Morison equation coefficients for the plate under a variety of sea-states are obtained and used in numerical models to determine the platform response and pressure distribution on the hull.

## Applications

With increasing exploration activities from offshore basins, such as the Gulf of Mexico, numerous discoveries of relatively small hydrocarbon accumulations have taken place. Many of these fields do not contain sufficiently large amount of oil and or gas to justify the expenses of a stand-alone field development, such as a production platform and pipeline infrastructure. In many instances, however, these fields can be produced using subsea-tiebacks to existing infrastructure. These include a subsea wellhead and a flowline to an existing production platform for example.

Serious limitations are expected with longer subsea tie-back, such as hydrate formation inducing plugging of the line due to a decrease in pressure and temperature along the flowline. Conventional remedial measures include heated flowlines or injection of chemicals to prevent the formation of hydrates. Such chemicals can be transported from the host platform to the subsea wellhead in an umbilical, and can be injected into the flowline at the wellhead. The umbilical can also be used to control the subsea wellhead. The cost of such umbilical is typically very large, and the economics of a subsea tie-back is often threatened by the excessive umbilical cost for tie-back distances greater than 20 miles. An alternative development scenario consists of providing a minimum offshore platform near the wellhead with remote control from the host platform and injection of chemical stored on the minimum offshore platform via a short umbilical connected to the subsea wellhead (Figure 2). The presence of a platform directly above the wellhead enables pig launcher capabilities and well logging tools support.

When multiphase hydrocarbon flow is expected, the tie-back distance is limited because of flow assurance problems. Current technological developments are aimed at providing subsea separation facilities to allow hydrocarbons to flow over a greater distance. Such subsea facilities may require additional surface facilities such as power generation and complex control capability.

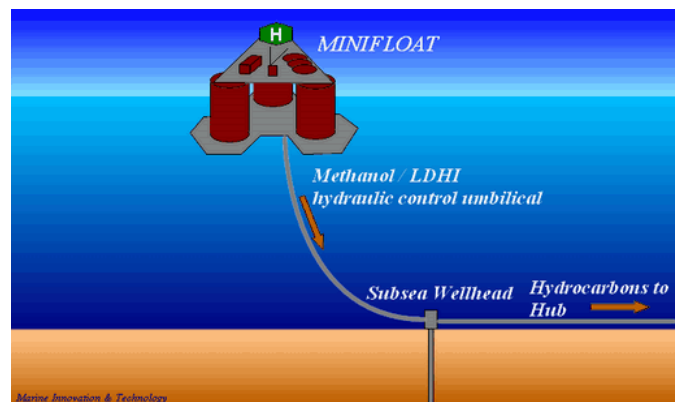


**Figure 2: Chemical injection**

Similarly, equipment such as subsea pumps may be required to assist flow assurance over the tie-back length. Such pump requires power which can be provided by a surface facility located above the pump (Figure 3).

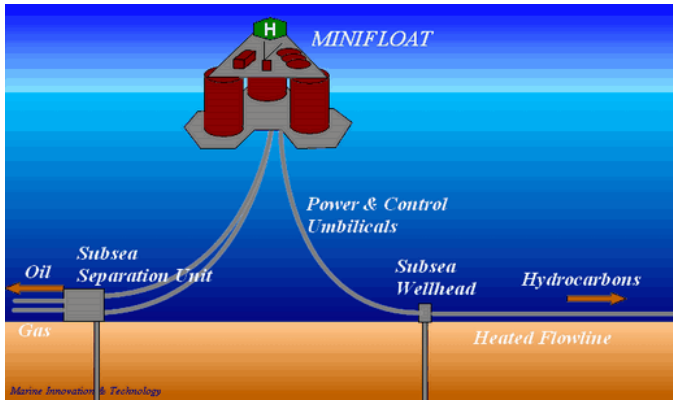


**Figure 3: Power generation & control center**

Other technological solutions provided to the flow assurance problem for extended tie-back include electrically heated flowline, which may be heated either continuously or before start-up. The power required to heat the flowline may be produced by a generator located on minimum offshore facilities floating above the flowline.

Current technologies allow certain processing operations to be performed using much smaller equipment than traditional technologies. A minimum offshore platform could therefore be used to perform operations currently conducted on much larger platforms such as first and second stage separation. This could further extend the distance over which hydrocarbons can be transported allowing them in cases to reach the shore directly for further processing (Figure 4).

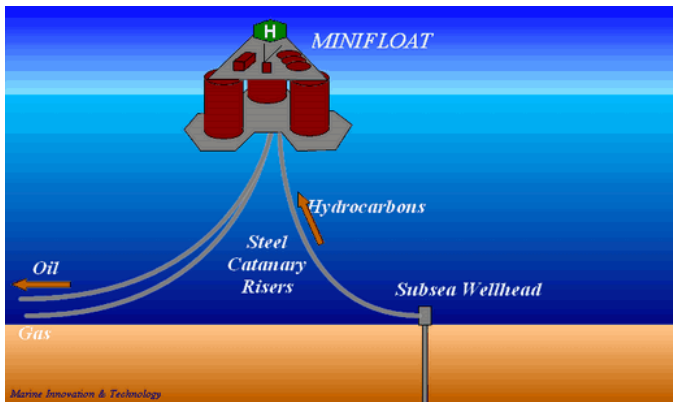


**Figure 4: Separation.**

It is envisioned that future technologies such as fuel cell conversions could be conducted on minimum offshore facilities and power could be shipped via an electrical cable back to shore. A minimum offshore platform can also be used to perform basic maintenance workover on the wellhead by providing support for coil tubing applications. This saves the high cost of mobilization of a vessel suitable for typical work over operation.

Water treatment and reinjection can be performed economically using a minimal offshore platform (Figure 5) for fields requiring pressure maintenance.

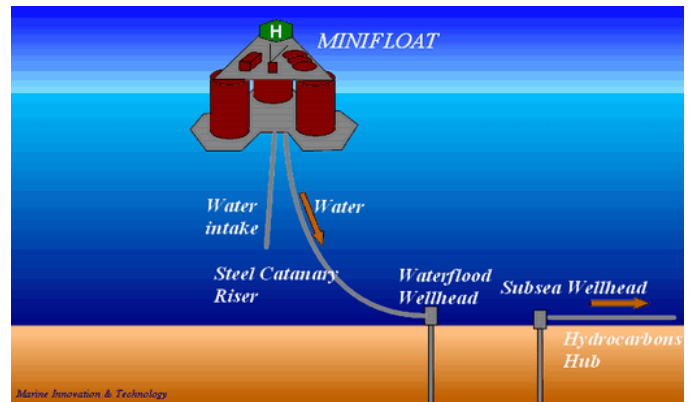


**Figure 5: Waterflood wells.**

Therefore, advancing subsea and surface processing technologies combined with a low cost minimum offshore platform will considerably enhance profitability and technical feasibility of deepwater marginal fields.

### Cost estimate

The cost of this floater is low in part because of the simplicity of the platform design and its minimal size, but also because of the ease of construction, deployment and installation of the complete system. A gulf-coast shipyard construction is envisioned for applications in the Gulf of Mexico, with onshore integration. The complete platform is towed to site, where the mooring system has been preinstalled with a small anchor-handling vessel. No expensive transportation, upending and offshore deck mating are necessary. Cost estimates of two MINIFLOAT configurations in 6,000 ft waterdepth are provided in table 1. The “small size” MINIFLOAT, with a total displacement of 1,600 tons, is designed to control a subsea wellhead and inject chemicals into the flowline. The “medium size” system, with a 5,500 tons displacement, supports an unmanned water injection facility. The 1,600 tons configuration is the smallest system capable of surviving the GOM 100 year storm. (No green water on deck). The 5,500 tons system is the concept used in the analysis below.

**Table 1: MINIFLOAT cost estimate**

MINIFLOAT size	Small	Medium
Displacement (st)	1,600	5,500
Column diameter (ft)	25	38
Draft + air gap (ft)	60	90
Payload (st)	700	2,600
Cost		
Hull (k\$)	3,943	15,918
Mooring (k\$)	1,026	4,154
Umbilical / riser (k\$)	900	900
Installation (k\$)	4,140	6,270
<b>Total (k\$)</b>	<b>10,009</b>	<b>27,242</b>

The hull cost includes hull appurtenances and deck steel. Equipment cost is not included.

Mooring cost include the anchors, the wire or polyester line, wire,

chains and connectors. The offshore installation cost includes the towing, pre-lay, mooring line connection, riser / umbilical pull-in and commissioning. Most of these operations are done with small vessels. The riser pull in require a larger vessel (more expensive day rate), but this operation can be conducted while the particular ship is mobilized for a well operation or flowline installation.

## DESIGN METHODOLOGY

A suite of numerical tools are developed for the design of the floating platform. From the field characteristics, a list of necessary equipment, storage capacity and power requirement is identified. This defines the platform payload. The metocean criteria are also required.

A spreadsheet is then used to size the platform. This sizing tool generates the platform design and performs preliminary verification of stability, global structural requirements, dynamic characteristics, platform offset and mooring tensions. The floater main characteristics including GM, Cg, and mass matrix are obtained from this analysis and used as an input to a time-domain motion analysis software which predicts the motions of the floater in a given sea state. Operational and survival criteria are defined and checked against the time-domain results. Results are then fed back into the sizing spreadsheet until convergence is achieved.

## NUMERICAL ANALYSIS

The response of the floater described in this paper is obtained in the time-domain because significant non-linear effects are expected, which make a frequency-domain approach more uncertain. Both the mooring system and the large viscous effects on the water-entrainment plate have significant non-linear terms. A time-domain motion analysis solver is developed to predict the platform motion in any sea-state. This solver (TIMEFLOAT) solves Newton equations of motion. The vessel and mooring responses are fully coupled through a time-marching scheme. Wave loads are modeled using a linear diffraction-radiation solver and viscous effects on the water-entrainment plate using a modified Morison equation model. More details on the numerical model are presented in the next sections.

### Diffraction-radiation solution

The added mass, damping and wave exciting forces are obtained using the commercial diffraction/radiation code WAMIT. The hull panel model is presented in Figure 6.

An initial understanding of the floater response is obtained by computing the response amplitude operators (RAO) for the freely floating system. Large resonances are observed when the RAO are calculated with no other damping than the wave radiation component. These are not realistic, however, because viscous damping on the system significantly reduces resonances. An external damping matrix has therefore been empirically determined based on time-domain viscous results, presented in a later section. RAO have been calculated with the external damping matrix, in order to generate more realistic results. This damping matrix is only used in the present frequency-domain sensitivity analysis, but not in the time-domain simulations.

The water-entrainment plate is a stiffened shell approximately one inch thick with structural members. It is modeled as a flat element with

finite thickness. Numerical convergence problems are experienced when modeling the plate with a sink/source distribution because, as the thickness reduces, the solution becomes singular. The required number of panels increases considerably as the plate thickness get small compared to its span. To quantify the effect of plate thickness on the motion prediction results, a dipole formulation is used to obtain the asymptotic solution. One recalls that the dipole formulation is used for infinitely thin plates (Lamb 1932, Newman, 1977).

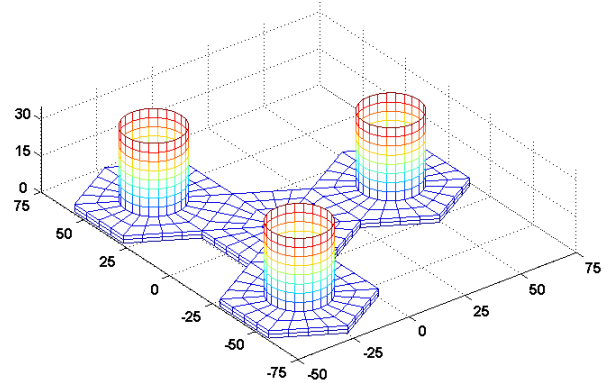


Figure 6: Example of grid used in the hydrodynamic calculations.

Figure 7 shows how the solution converges as the thickness of the plate gets smaller. The RAO shown correspond to the floater geometry and mass properties defined in the results section. The heave RAO converges rapidly with decreasing plate thickness. However, the pitch results require a thinner plate. The solution obtained with a 0.75 ft thick plate is within 5% of the “converged” dipole solution.

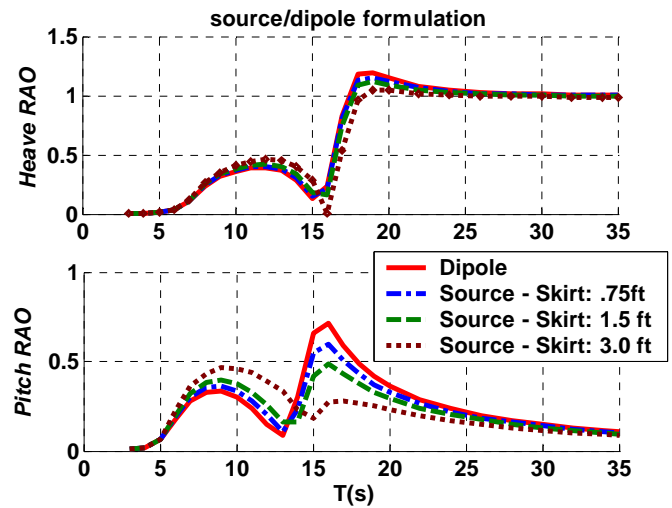


Figure 7: Numerical sensitivity on plate thickness

A large horizontal plate close to a free surface can have the effect of increasing the wave exciting force. The consequence on the motion response is however largely offset by the additional damping created by the plate and the shifting of the platform natural response away from the GOM wave energy due to the significant increase in the added mass

term. The response of the equivalent 3-columns semi-submersible without the heave plate is plotted in Figure 8 against the corresponding MINIFLOAT configuration with water-entrapment plate. The plate is an integral part of the platform and its sizing is used in the design process to influence the motion response. Without it, the only variables that can be adjusted are the column spacing and diameter, quantities intrinsically linked to the platform hydrostatics. For example, to increase the natural period, one would have to reduce the column diameter. This would force a significant increase in draft and would have substantial repercussions on the overall stability, structural behavior and cost. An additional benefit of the plate is its stabilizing effect due to the large weight placed at the base of the platform.

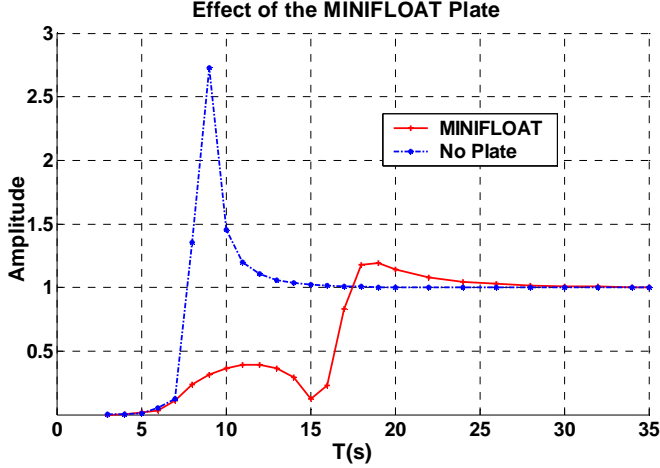


Figure 8: Heave RAO in head sea with (solid red) and without (dash blue) the bottom plate.

## Time-domain formulation

Time-series of the environmental loading on the platform are based on the linear-superposition of incident waves, and wind spectral components. Wind and wave frequency components and phases are randomized to reduce the time-series auto-correlation. For instance, the wave height at the fixed origin is obtained from:

$$y = \sum_{k=1,N} a_k \cos(\omega_k t - \varphi_k) \quad (1)$$

where:

$\omega_k$  are the wave frequencies randomly distributed

$\varphi_k$  are the phases, randomly distributed between 0 and  $2\pi$

$a_k$  are the wave components at frequency  $\omega_k$ , such that

$$a_k^2 = \int_{\omega_1}^{\omega_2} S(\omega) d\omega$$

$\omega_1 = \frac{\omega_{k-1} + \omega_k}{2}$        $\omega_2 = \frac{\omega_k + \omega_{k+1}}{2}$

and

$S(\omega)$  is the wave spectrum

The vessel motion is obtained by solving Newton's equation of motion. It is assumed that the sea-state is relatively narrow-banded, and

therefore the added-mass and damping coefficient only varies slightly within one standard deviation on each side of the wave spectrum peak. Although this approximation is not strictly necessary, it speeds up considerably the computations by removing the need to calculate a convolution of the vessel velocity and acceleration with the retardation functions. Note that this approximation cannot be used to study slamming problems where the transient effects are highly frequency-dependent. The resulting Newton's equation of motion reads as follows:

$$[m + m_a(T_p)]\ddot{\bar{x}} + [d(T_p)]\dot{\bar{x}} + [k]\bar{x} = \bar{F}_d + \bar{F}_m + \bar{F}_v + \bar{F}_w + \bar{F}_{sd} \quad (2)$$

where:

$[m]$  is the mass matrix

$[m_a(T_p)]$  is the added-mass matrix at the frequency of the sea-state spectral peak

$[d(T_p)]$  is the wave damping matrix at the frequency of the sea-state spectral peak

$\bar{x}$  is the 6DOF vessel response

$\bar{F}_d$  is the wave diffraction force

$\bar{F}_m$  is the mooring and tether force

$\bar{F}_v$  is the viscous forces on the column and on the plate

$\bar{F}_w$  is the dynamic wind force

$\bar{F}_{sd}$  is the slow-drift force obtained from linear calculations using Newman's approximation.

The linear wave diffraction force  $\bar{F}_d$  is calculated as follows:

$$(\bar{F}_d)_i = \sum_{k=1,N} a_k f_i(\omega_k) \cos(k_x x + k_y y - \omega_k t - \varphi_k - \varphi_{ik}) \quad (3)$$

where

$$k_x = \frac{\omega^2}{g} \cos(\beta)$$

$$k_y = \frac{\omega^2}{g} \sin(\beta)$$

$\beta$  is the wave heading

$x, y$  are the vessel horizontal coordinates

$f_i(\omega_k), \varphi_{ik}$  are the diffraction force and phase in direction  $i$  per unit wave amplitude at frequency  $\omega_k$

The dynamic wind force is obtained in a similar manner by considering the dynamic wind velocity and the drag and lift coefficients of the structure. It is assumed that the vessel yaw oscillations are relatively small, and therefore the wind and diffracted wave coefficients correspond to a constant heading throughout the simulations. This approximation may not be suitable for the study of turret-moored Floating Production Storage Offloading vessels (FPSO), when large yaw variations are expected.

The solution to Equation 2 is obtained by a time-marching scheme based on Runge-Kutta algorithm. At each time step, the mooring system is solved using a relaxation method, and the vertical and horizontal line tensions are calculated. The viscous effects are obtained using modified Morison type elements, as described in the next section.

## Viscous model

Flow separation occurs downstream of the columns due to viscous interaction between the columns and the current and wave kinematics. As a result, additional loads, not computed by the linear diffraction-radiation theory are present. Morison equation is used to determine the viscous forces on the columns. Because the added-mass and wave inertia terms are accounted for in the diffraction-radiation solution, only the drag term is used. The columns are discretized in small viscous elements (line members, which are fixed with the body) on which the Morison equation is applied. The instantaneous location of the line members and wave kinematics at that location are calculated at every time step to determine the relative velocity between the body and the flow. The resulting viscous force is expressed as follows:

$$F_v = \frac{1}{2} \rho C_d D L U |U| \quad (4)$$

where  $U = \mathbf{t} \times (\mathbf{u}_C + \mathbf{u}_W - \mathbf{u}_B) \times \mathbf{t}$  is a vector component in a plane normal to the axis of the member and in a plane defined by the relative velocity and the line member axis.  $\mathbf{t}$  is a unit vector along the axis of the line member, and  $L$  is the length of the line member.

$\mathbf{u}_C$  is the current velocity,  $\mathbf{u}_W$  is the wave-induced velocity based on linear superposition and the Wheeler stretching method (Wheeler, 1969), and  $\mathbf{u}_B$  is the body velocity at the location of the line member. Numerical simulation were conducted with  $C_d=1.2$  on the columns.

Flow separation also occurs along the edges of the water-entrapment plate. Similarly, viscous elements with a Morison model (equation 4) are generated along the edges of the water-entrapment plate. The resulting viscous force is assumed to be normal to the plate, and therefore:

$U = [(\mathbf{u}_C + \mathbf{u}_W - \mathbf{u}_B) \cdot \mathbf{n}] \mathbf{n}$  where  $\mathbf{n}$  is a unit vector normal to the plate. The drag coefficient assumes that the overall plate drag coefficient based on the plate area is equal to 1.17 from high Reynolds steady flow measurements on square and circular plates by Hoerner (1965). The corresponding drag force on the line members at the edge of the plate is based on the ratio of the plate area to the line member length. For instance, in the simulations presented here, the line members at the edge of the water-entrapment plate assume a drag coefficient times diameter ( $C_d D$ ) term equal to 25.

Model tests are currently being performed to validate the viscous effects and calibrate the numerical tool. The model was towed at various speeds to investigate the plate-generated lift. The shape of the water-entrapment plate is optimized to not present a uniform leading edge to single current direction, and in all tow cases with and without angle of attack, no significant lift was observed.

The tow tests have also confirmed that this hull shape does not experience VIM, which was expected due to the multi-column design, with a large gap between columns and a short column length.

## Mooring system

A two-dimensional finite difference scheme (Chatjigeorgiou, 1998) is implemented to solve the mooring line equations using a cable dynamics model. The nonlinear ordinary differential equations are solved at every time step using a relaxation method. A friction model

is implemented on the sea-bed. The mooring line configuration between the vessel fairlead and the touch-down point is solved iteratively, until bottom tension and touch-down location are converged. The top tension is calculated on each mooring line, and fed into the Newton's equation of motion for the floater (equation 2).

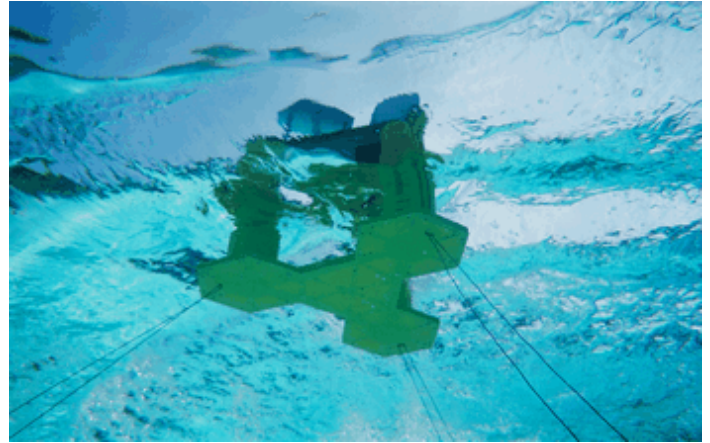


Figure 9: Photograph of model during model tests

## Validation of software tool

Systematic validations of the software results were performed for various mooring configurations (taut, semi-taut, catenary, buoyancy modules). Tensions and mooring configurations were compared with the results of a finite-element solver. Sample comparisons are provided in Figure 10, which shows the mooring tension response for a catenary (Fig 10a) and taut (Fig 10b) mooring system. In both cases the agreement is very good. The mooring system in this case is composed of wire with the following properties: EA=1.0E8 lbs, w=30 lbs/ft, wb=5 lbs/ft, length=8,000 ft, waterdepth=5,000 ft.

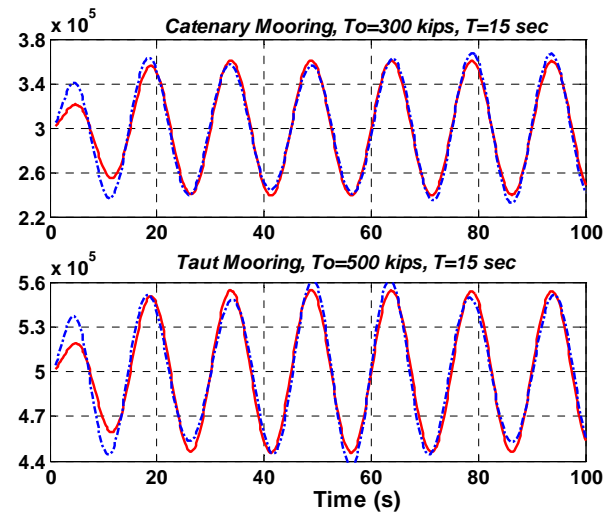


Figure 10 a & b: Mooring tension response validation using timefloat (solid red) and a commercial tool (dash blue).

## RESULTS

The following section describes the response for a MINIFLOAT platform whose characteristics are described in Table 2.

**Table 2: Platform specification**

Design Basis	
Water depth	6000ft
Metocean	GOM
Sizing	
Spacing between Column	80 ft
Column diameter	38 ft
Draft	50 st
Still water airgap	40 st
Distance from center of column to edge of plate	39.3 ft
Water entrapment plate area	16,000 ft <sup>2</sup>
Weights	
Displacement	5,500 st
Topsides (deck steel, equipment, riser and umbilical tension)	2,100 st
Fluids on board	500 st
Mooring	
Mooring lines diameter (EIP-wire)	2.75 in
Mooring line MBL	360 st
Top tension on each line	75 st

### Response Amplitude Operators

For the specific case above, the 5,500 tons MINIFLOAT platform motion response (dash blue in figure 11) is compared against a 3<sup>rd</sup> generation semi with 28,000 tons displacement (solid red in figure 11). These RAO have been obtained from the ratio of the motion rms in time domain to the rms of a regular wave train. We note that the viscous and non-linear mooring responses are included in this “RAO” formulation.

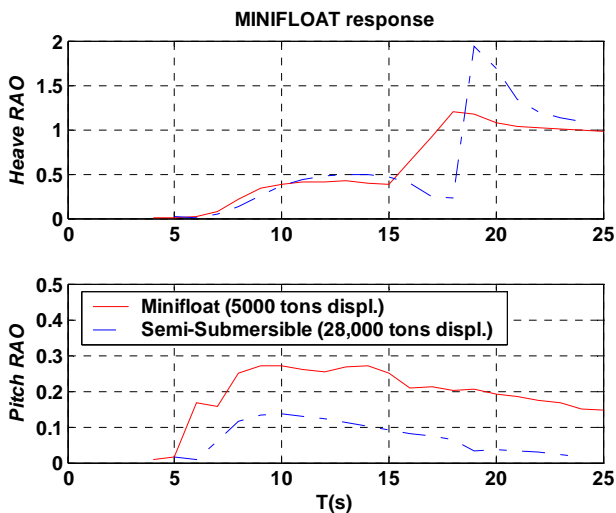


**Figure 11a & b: Non-linear equivalent RAO comparison between a 5,000 tons displ. Minifloat (solid red) and a 28,000 tons displ. 3<sup>rd</sup> generation semi-submersible (dash blue).**

The heave response of the two floaters is very similar in magnitude,

although the MINIFLOAT displacement is 5 times smaller than that of the semi-submersible platform. The pitch response of the new concept presented here is larger than that of the much larger semi-submersible, which is expected, since the semi-submersible column spacing is significantly larger.

**Table 2: Platform response in various sea-states**

Hs=10 ft, Tp=8 s	mean,	rms,	max,	min,
offset (ft)	-8.0	1.7	-3.3	-13.9
heave (ft)	0.1	0.5	1.7	-1.8
pitch (deg)	0.4	0.5	2.6	-1.2
tension (kips)	167.7	3.0	178.2	160.9
Hs=15 ft, Tp=10 s	mean,	rms,	max,	min,
offset (ft)	-9.1	3.2	-0.4	-23.8
heave (ft)	0.1	1.1	3.3	-4.6
pitch (deg)	0.4	0.9	4.9	-2.2
tension (kips)	170.0	5.9	196.7	153.6
Hs=41 ft, Tp=14 s	mean,	rms,	max,	min,
offset (ft)	-71.0	15.6	-36.8	-141.3
heave (ft)	-0.4	6.0	16.9	-22.1
pitch (deg)	3.4	3.6	15.7	-6.5
tension (kips)	316.7	38.3	498.1	228.9

However, time-domain simulations have shown that the pitch response of MINIFLOAT is sufficient to satisfy stringent operational criteria:

- it has been assumed that safe helicopter landing can be conducted with maximum platform rotation of 2.5 deg (including mean and dynamic components). Corresponding rotations are obtained in a 10 ft sea-state with 8 second peak period, as shown in Table 3.
- The platform equipment can be operated without problem up to maximum rotations of 5 degrees. As per Table 3, this condition arises in 15 ft significant waves with 10 second period.

Corresponding operability has been determined based on the occurrence of sea-states in the Gulf of Mexico. It is plotted as a function of the month in Figure 12. Helicopter landing is possible 96.4% of the time on an annual basis, and equipment operation with less than 5 deg pitch is possible 99.7% of the time, yearly average. Maximum rotations in a 100 year hurricane are approximately 15 degrees. Heave rms is substantial in extreme storms, which allow the platform to “ride the wave”, and reduce the risk of wave impact on the deck.

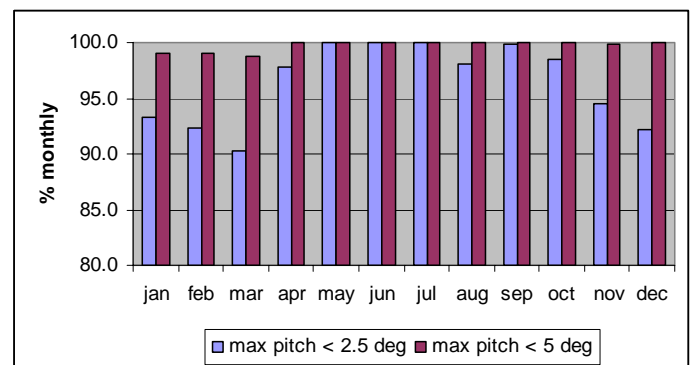


**Figure 12: Operability of the MINIFLOAT platform in the Gulf of Mexico, based on a 2.5 deg, and 5 deg max pitch response**

## CONCLUSIONS

A new concept of minimal floating offshore platform is presented in this paper. This platform aims at enabling the development of marginal fields in deep and ultra-deepwater. It provides a surface support for primarily subsea development. The platform offers excellent motions characteristics, and by optimizing equipment placement between the sea bed and the surface, this new structure is key to reducing cost of marginal developments.

This platform is:

- Cheaper and smaller than 3rd generation semi-submersibles;
- More versatile than a control buoy, and provides more usable deck space than competing concepts.
- It enables many subsea development scenarios at onset by giving operators options in adding functionality later during the life of the development.

The simplicity of design, construction and installation along with technology advances in subsea and surface process equipment can substantially reduce development costs for deep and ultra deepwater marginal fields.

A fully coupled non-linear mooring time-domain motion analysis tool is developed to predict the motions of this platform. The water-entrapment plate viscous effects are modeled, and the mooring solution is coupled at every time step with the platform response. The analysis performed shows that for a 5,500 tons displacement case, the motions are acceptable, with a heave response similar to the one of a much larger semi-submersible, and a pitch response acceptable for stringent operational criteria, such as helicopter landing.

Model tests are currently being conducted to validate the concept and to calibrate the viscous model presented here. Validations with other software show that the mooring responses are well predicted.

## REFERENCES

ABS Press Releases, November (2003). "ABS Provides Its First Guidance on Building, Classing TLPs, Spars", ABS addresses global performance issues in supplement to *Guide on Building, Classing Floating Production Installations*

- Chatjigeorgiou I.K. and Mavrakos S.A. (1998) "Assessment of bottom-cable interaction effects on mooring line dynamics" *17<sup>th</sup> Intl. Conf. Offsh. Mech. Arctic Engrg.* OMAE98-0355.
- Energy Information Administration, (2003). "48 U.S. Crude Oil, Natural Gas", *Gas Liquids Reserves 2002 Preliminary Annual Report*.
- Faltinsen, O.M. (1990). "Sea Loads on Ships and Offshore Structures", *Cambridge Ocean Technology Series*, Cambridge University Press
- Hoerner S.F. (1965). "Fluid dynamic drag" *Hoerner Fluid Dynamics*
- Holmes, S. Bhat,S., Beynet P., Sablok, A. and Prislin, I., (2001). "Heave Plate Design With Computational Fluid Dynamics" *Journal of Offshore Mechanics and Arctic Engineering* , Volume 123, Issue 1, pp. 22-28
- Lamb, H. (1932). "Hydrodynamics" 6<sup>th</sup> Ed. Cambridge: Cambridge University press. Reprinted 1945, New York: Dover.
- Newman, J. N. (1977). "Marine Hydrodynamics", MIT Press, Cambridge Massachusetts.
- O'Kane, J.J., Troesch, A.W. and Thiagarajan, K.P. (2002). "Hull component interaction and scaling for TLP hydrodynamic coefficients", *Ocean Engineering*, 29:8018, pp 513-532
- Shell Press Release (October 2003) "Shell Global Solutions Announces Fairings to Reduce Vortex Induced Vibration Slated for Deepest TLP"
- Tao, L., Thiagarajan, K. and Cheng, L. (2000). "On Parametric Dependence of Springing Damping of TLP and Spar Columns". *Applied Ocean Research*, **22** (5), pp.281-294.
- Thiagarajan, K.P., Ran, A., Tao, L., Datta, I. and Halkyard, J. (2002). "Influence of Heave Plate Geometry on the Heave Response of Classic Spars", *21st International Conference on Offshore Mechanics and Arctic Engineering*, New York, ASME, pp 1-7
- Wheeler, J.D. (1969). "Method of calculating forces produced by irregular waves", *Proc. First Offsh. Tech. Conf. OTC 1006*, Houston